Fermentable carbohydrate stimulates FFAR2-dependent colonic PYY cell expansion to increase satiety

CrossMark

Lucy Brooks [1],[9], Alexander Viardot [4],[9], Anastasia Tsakmaki [2], Emilie Stolarczyk [2], Jane K. Howard [2], Patrice D. Cani [5], Amandine Everard [5], Michelle L. Sleeth [1], Arianna Psichas [1], Jelena Anastasovskaj [3], Jimmy D. Bell [3], Kim Bell-Anderson [6], Charles R. Mackay [7],[8], Mohammad A. Ghatei [1], Stephen R. Bloom [1], Gary Frost [1],**,[10], Gavin A. Bewick [1],[2],*,[10]

ABSTRACT

Objective: Dietary supplementation with fermentable carbohydrate protects against body weight gain. Fermentation by the resident gut microbiota produces short-chain fatty acids, which act at free fatty acid receptor 2 (FFAR2). Our aim was to test the hypothesis that FFAR2 is important in regulating the beneficial effects of fermentable carbohydrate on body weight and to understand the role of gut hormones PYY and GLP-1.

Methods: Wild-type or $Ffar2^{-/-}$ mice were fed an inulin supplemented or control diet. Mice were metabolically characterized and gut hormone concentrations, enteroendocrine cell density measurements were carried out. Intestinal organoids and colonic cultures were utilized to substantiate the *in vivo* findings.

Results: We provide new mechanistic insight into how fermentable carbohydrate regulates metabolism. Using mice that lack FFAR2, we demonstrate that the fermentable carbohydrate inulin acts via this receptor to drive an 87% increase in the density of cells that produce the appetite-suppressing hormone peptide YY (PYY), reduce food intake, and prevent diet-induced obesity.

Conclusion: Our results demonstrate that FFAR2 is predominantly involved in regulating the effects of fermentable carbohydrate on metabolism and does so, in part, by enhancing PYY cell density and release. This highlights the potential for targeting enteroendocrine cell differentiation to treat obesity.

1. INTRODUCTION

Obesity is currently one of the most serious global threats to human health and an important modifiable risk factor for type-2 diabetes, hypertension, and certain cancers [1—3]. Susceptibility to obesity is determined by genetic background, diet, and lifestyle. Additionally, over the past decade, it has become apparent that the resident intestinal microbiota also plays an important role in determining susceptibility to obesity [4—7]. This is partly due to the production of physiologically active metabolites during the process of microbial fermentation, which serve to harvest energy from dietary substrates that would otherwise be lost in the feces [8,9]. This is typified by the fermentation of non-digestible carbohydrates, which, when supplemented into the diet, reduce appetite and body weight gain and improve glucose homeostasis in rodents and humans [10—12]. Key metabolites involved in transducing these beneficial metabolic effects are the short-chain fatty acids (SCFAs) acetate, propionate and butyrate [8]. Indeed, recent evidence suggests that the increased production of propionate following gastric bypass surgery for obesity is related to weight loss [13].

[1]Division of Diabetes, Endocrinology and Metabolism, Imperial College London, London, W12 0NN, UK [2]Division of Diabetes and Nutritional Sciences, King's College London, London, SE1 9RT, UK [3]Metabolic and Molecular Imaging Group, MRC Clinical Science Centre, Imperial College London, London, W12 0NN, UK [4]Diabetes & Metabolism Division, Garvan Institute of Medical Research, Sydney-Darlinghurst, NSW, 2010, Australia [5]Louvain Drug Research Institute, Metabolism and Nutrition Research Group, WELBIO (Walloon Excellence in Life sciences and BIOtechnology), Université catholique de Louvain, B-1200, Brussels, Belgium [6]School of Molecular Bioscience, University of Sydney, Sydney, NSW, 2006, Australia [7]Charles Perkins Centre, Sydney Medical School, University of Sydney, Sydney, NSW, 2006, Australia [8]Department of Immunology, Monash University, Clayton, VIC, 3800, Australia

[9] Lucy Brooks and Alexander Viardot contributed equally to this work.

[10] Gary Frost and Gavin A. Bewick contributed equally to this work.

*Corresponding author. Division of Diabetes and Nutritional Sciences, King's College London, London, SE1 9RT, UK. E-mail: gavin.bewick@kcl.ac.uk (G.A. Bewick).

**Corresponding author. Division of Diabetes, Endocrinology and Metabolism, Imperial College London, London, W12 0NN, UK. E-mail: g.frost@imperial.ac.uk (G. Frost).

While SCFAs can be utilized for *de novo* synthesis of lipids and glucose [14] and serve as an energy source, they also act as signaling molecules at the recently de-orphaned G-protein coupled receptors, free fatty acid receptor 2 (FFAR2, also known as GPR43) and FFAR3 (also known as GPR41) [15,16]. Both receptors are expressed in various peripheral tissues, including the gastrointestinal tract, pancreas, bone marrow, spleen, thymus, lung, breast, and white adipose tissue; therefore, SCFAs may have widespread effects [15,17—20].

Within the gastrointestinal tract, FFAR2 and 3 have been localized to enteroendocrine L cells [17]. These specialized gut cells secrete the anorectic hormone peptide YY (PYY) and the incretin glucagon-like peptide-1 (GLP-1) in response to luminal nutrients, such as sugars, amino acids, and long-chain fatty acids [17,21,22]. The highest density of L cells is found in the colon where these nutrients are unlikely to reach significant concentrations, but where SCFAs are most concentrated [23]. This suggests that gut hormone release may be an important host response to microbial fermentation and the consequent production of SCFAs. In support of this, acetate and propionate have been shown to stimulate the secretion of GLP-1 *in vitro*, an effect which was attenuated by FFAR2 deletion [24]. We therefore hypothesize that SCFA activation of L cell-expressed FFAR2, contributes to the effects of microbial fermentation on host metabolism.

To determine if the beneficial metabolic effects of fermentable carbohydrate are mediated by FFAR2 signaling, we used mice with targeted deletion of this receptor. We demonstrate for the first time that this receptor is essential for mediating inulin's ability to reduce food intake and protect against diet-induced obesity. FFAR2 signaling was found to drive an expansion of the PYY cell population within the colon, leading to increased circulating PYY, thus potentiating anorectic signaling by the gut. Our findings suggest that the fermentable carbohydrate stimulated expansion of PYY-expressing cells within the proximal colon is a physiologically important pathway linking diet, gut microbiota, and host metabolism.

2. METHODS AND MATERIALS

2.1. Study approval

All animal procedures were approved by the local ethical review process and the British Home Office Animals Scientific Procedures Act 1986 and carried out at Imperial College London (project license numbers: 70/7096, 70/7236 and 70/7595) or the Garvan Institute of Medical Research (12_22).

2.2. Animals and diets

Male $Ffar2^{-/-}$ C57BL/6 mice were obtained from Deltagen (http://wwww.deltagen.com). The *Ffar2* gene was deleted by homologous recombination, which substitutes 55 bp of *Ffar2* exon 1 with the β-gal-neo cassette, shifting the downstream amino acid sequence out of the reading frame [25]. Mice were maintained in cages under controlled temperature (21—23 °C) and light (12 h light/12 h dark) with *ad libitum* access to food and water. $Ffar2^{-/-}$ and WT littermates at 9 weeks of age were fed a high-fat "Western" diet containing 21% anhydrous milk-fat and 34% sucrose, supplemented with 7.5% inulin (HFI) or an isocaloric control diet supplemented with 3.3% cellulose + 4.2% corn starch (HFC) for 14 or 2 weeks. For analysis of proliferation, Bromodeoxyuridine (2.6 mM) was administered in the drinking water for the second week of the 2-week intervention. Investigators were blinded to the sample group allocation during the experiment and analysis.

2.3. Magnetic resonance imaging

Adiposity was quantified by MRI following 13 weeks dietary intervention. Mice were anesthetized using 3% isoflurane in oxygen at a flow-rate of 2 L/min and scans acquired on a 4.7 T Varian INOVA imaging system (Varian) using a quadrature birdcage coil [26].

2.4. Intra-peritoneal glucose tolerance and insulin tolerance tests

Glucose and insulin tolerance tests were performed immediately prior to dietary intervention and following 11 and 12 weeks intervention, respectively. For glucose tolerance tests $Ffar2^{-/-}$ and WT C57BL/6 mice were fasted for 14 h then injected intra-peritoneally (i.p.) with 2 g/kg glucose. For insulin tolerance tests, mice were fasted for 5 h then i.p. injected with 1 IUkg^{-1} insulin (Humulin 100 IUml^{-1}). Blood glucose measurements were taken via tail bleed using a glucometer (Bayer contour®).

2.5. Energy expenditure and physical activity

Energy expenditure and physical activity were determined in 14-week old $Ffar2^{-/-}$ and WT C57BL/6 mice fed HFC or HFI diet for 4 weeks. Animals were transferred to individual cages in an open-circuit calorimeter (Oxymax Series; Columbus Instruments, Columbus, OH, USA). Temperature was maintained at 22 °C, with airflow of 0.6 L/min. Mice were acclimatized to the cages for 24 h before beginning 24-h recording of oxygen consumption (VO$_2$) and carbon dioxide production (VCO$_2$). Energy expenditure (kilocalories of heat produced) was calculated as calorific value (CV) × VO$_2$, where CV = 3.815 + 1.232 × RER as previously published [27]. Physical activity was also measured, using an OPTO-M3 sensor system (Columbus Instruments, Columbus, OH, USA), whereby ambulatory counts were a record of consecutive adjacent photo beam breaks in the horizontal space (X and Y axis). Data were presented as hourly averages for energy expenditure as well as hourly summation for ambulatory activities. The calorimeter was calibrated before each use using highly pure primary gas standards (O$_2$ and CO$_2$).

2.6. Fecal mass and energy content

Fecal matter was collected over four days. Energy content in the feces was determined in duplicate using a bomb calorimeter (PARR 1356; John Morris Scientific Pty Limited, Australia). Briefly, feces was compressed, pelleted (PARR Instrument Company; Moline, IL, USA), and weighed. Pellets were frozen and then freeze-dried (Telstar Cryodos −80 °C freeze dryer, Progen Scientific, UK) for 24 h. Each pellet was re-weighed to determine moisture content, placed in the bomb calorimeter for combustion, and energy content determined against a standard (benzoic acid).

2.7. Quantitative enzymatic determination of glycerol

Quantitative enzymatic determination of glycerol was carried out using Free Glycerol Reagent (Sigma—Aldrich) following alkaline hydrolysis of triglycerides to glycerol and free fatty acids. Triplicate samples were diluted 1/5 and 10 μl was used for analysis.

2.8. Tissue collection

Anesthetized mice were sacrificed by decapitation following a 4 h fast. Blood was collected into heparinized syringes and transferred to tubes containing 15 μl Trasylol (10,000 K IUml^{-1}) (Nordic Pharma) and 10 μl dipeptidyl peptidase IV (DPP-IV) inhibitor KR-62436 hydrate (2.7 mM) (Sigma). Colonic tissue for immunohistochemistry was fixed in Bouin's solution overnight at 4 °C and then paraffin embedded. Tissue samples for protein or triglyceride analysis were snap frozen in liquid nitrogen

and stored at −80 °C. Samples for RNA analysis were stored in RNA*later*™ (QIAGEN).

2.9. Biochemical analyses

LPS concentration in portal vein blood collected under terminal anesthesia was measured by using Endosafe-MCS (Charles River Laboratories) based on the Limulus Amebocyte Lysate (LAL) kinetic chromogenic methodology as previously described [28].

2.10. DNA isolation from mouse colonic samples

The colonic content of mice collected *post mortem* was stored at −80 °C. Metagenomic DNA was extracted using a QIAamp-DNA stool mini-kit (Qiagen) according to manufacturer's instructions. The primers and probes used to detect total bacteria, *Bifidobacterium* and *Lactobacillus* spp., were based on 16S rRNA gene sequences (Table 1) Detection was achieved with a STEP one PLUS instrument and software (Applied Biosystems) using MESA FAST qPCR MasterMix Plus for SYBR Assay (Eurogentec). Each assay was performed in duplicate in the same run. The cycle threshold of each sample was then compared to a standard curve (performed in triplicate) made by diluting genomic DNA (five-fold serial dilution) (BCCM/LMG and DSMZ). The data were expressed as Log bacteria/g of colonic content.

2.11. Quantitative PCR

Total RNA was isolated using TRI reagent (Sigma). Quantification and integrity analysis of total RNA was performed by running 1 μl of each sample on an Agilent 2100 Bioanalyzer (Agilent RNA 6000 Nano Kit, Agilent). RNA was purified using an RNeasy Mini Kit (Qiagen) and reverse transcribed using a high-capacity cDNA reverse transcription kit (Life technologies). Gene expression of *POMC*, *NPY*, *AgRP*, *Pax4*, *Pax6*, *Foxa1*, and *Foxa2* was quantified using 7900HT Fast Real-Time PCR System and TaqMan fluorogenic detection system (Applied Biosystems). Validated primers were purchased from Applied Biosystems. Comparative real-time PCR was performed in triplicate and data was analyzed according to the $2^{-\Delta CT}$ method normalized to 18S.

Real-time PCRs of *ZO1* and *Occludin* were performed with the StepOnePlus™ real-time PCR system and software (Applied Biosystems) using Mesa Fast qPCR™ (Eurogentec) for detection according to the manufacturer's instructions. RPL19 RNA was chosen as the housekeeping gene. All samples were run in duplicate and data were analyzed according to the $2^{-\Delta CT}$ method. The identity and purity of the amplified product was checked through analysis of the melting curve carried out at the end of amplification. Primer sequences for the targeted mouse genes are presented.

2.12. Organ culture

Fresh perigonadal WAT and subcutaneous WAT fat pads (∼100 mg) were cultured in 1 ml of RPMI serum free medium for 24 h as previously described [29]. Cytokines secreted were measured after 24 h by specific TNF-α ELISA (DuoSet ELISA Development kit, R&D, and ELISA Ready-SET-Go, eBioscience). Data are shown as the concentration of cytokines secreted in 1 ml of culture medium per gram of fat.

2.13. Isolation of mononuclear cells and flow cytometry

The stromal vascular fraction (SVF) containing mononuclear cells and pre-adipocytes was extracted from adipose tissue as previously described [29] and cells were stained with antibodies conjugated to fluorochromes, CD45 (30-F1), CD3 (145-2C11), CD4 (GK1.5), CD8 (53−6.7), NKp46 (29A1.4), B220 (RA3-6B2), CD11b (M1/70), F4/80 (BM8) (eBiosciences). 7-Amino-actinomycin D (eBiosciences) or LIVE/

DEAD Fixable Dead Cell Stain (Invitrogen) were utilized to discriminate between live and dead cells. Samples were acquired using a LSRII cytometer (Becton Dickinson) and data were analyzed using FlowJo software (Tree Star).

2.14. Quantification of gut hormone concentrations

Peptides were extracted from colonic tissue in boiling 0.5 mol L^{-1} acetic acid for 15 min. Colonic PYY, GLP-1, and substance P concentrations were determined using established in-house radioimmunoassays [30]. The concentration of glucose-dependent insulinotropic polypeptide (GIP) was measured using a commercially available kit (Merck Millipore). Similar to colonic peptide levels, circulating and portal vein GLP-1 and PYY concentrations were determined using in-house radioimmunoassays. Circulating leptin was measured using a commercially available kit (Merck Millipore).

2.15. Primary mixed colonic culture secretion experiments

WT and *Ffar2*$^{-/-}$ mice aged 8−10 weeks were killed by CO_2. Colons were collected and cleaned in ice-cold Leibovitz-15 medium (PAA). Tissue was digested with 0.4 mgml^{-1} Collagenase-XI (Sigma) in high glucose Dulbecco's modified Eagle's medium (DMEM) (10% fetal calf serum, 100 Uml^{-1} penicillin, and 0.1 mgml^{-1} streptomycin) at 37 °C as previously described [31]. Cell suspensions were centrifuged (5 min, 300 ×*g*) and the pellets re-suspended in DMEM. Cell suspensions were filtered through a nylon mesh (pore size ∼250 μm) and plated onto 24-well, 1% Matrigel-coated plates and incubated overnight at 37 °C in 95% O_2 and 5% CO_2.

Secretion studies were performed 24 h after culture preparation. Cultures were washed with secretion buffer (4.5 mM KCl, 138 mM NaCl, 4.2 mM NaHCO₃, 1.2 mM NaH₂PO₄·2H₂O, 2.6 mM CaCl₂, 1.2 mM MgCl₂, 10 mM HEPES, 0.1% fatty acid-free BSA) and incubated with 50 mM SCFA (acetate:propionate:butyrate 60:25:15) in secretion buffer for 2 h at 37 °C. Supernatants were collected and centrifuged. Cells were treated with lysis buffer containing: 50 mM Tris−HCl, 150 mM NaCl, 1% IGEPAL-CA 630, 0.5% deoxycholic acid, and one tablet of complete EDTA-free protease inhibitor cocktail (Roche). PYY and GLP-1 were assayed in supernatants and cell extracts by radioimmunoassay as previously described [32,33]. Hormone secretion was expressed as a fraction of the total of that hormone.

2.16. Immunofluorescence and microscopy

7 μm wax embedded sections were stained for PYY using primary polyclonal rabbit anti-PYY (1:1000, Abcam, ab22663), with secondary FITC-conjugated chicken anti-rabbit antibody (1:200, Abcam, ab6825). Staining for GLP-1 was carried out using primary polyclonal mouse anti-GLP-1 with secondary TRITC-conjugated goat anti-mouse (1:200, Abcam, ab5867). BrdU was stained for using primary monoclonal mouse anti-BrdU (1:100, Sigma, 13843420001) with secondary TRITC-conjugated polyclonal goat F(Ab) anti-mouse (1:200). 5HT was stained for using primary goat anti-5HT (1:500 Abcam, ab66047) with polyclonal donkey anti-goat (1:50, Abcam, ab6566). Nuclei were stained with DAPI (4′,6-diamidino-2-phenylindole) in Fluroshield (Abcam). Immunofluorescent images were acquired on a Carl Zeiss Axiovert 100S TV microscope. The operator performing the cell-counting was blinded to the groupings.

2.17. PYY-GFP organoid culture and treatments

Mouse intestinal crypts from transgenic PYY-GFP mice (a kind gift from Prof. Rodger Liddle, Duke University) [34] were isolated, cultured, and grown into organoids as described previously [35].

Crypts were cultured in advanced Dulbecco's modified Eagle's medium/F12 containing 100 units/mL penicillin/streptomycin, 10 mM HEPES, 2 mM Glutamax, supplements N2 ($1\times$) and B27 ($1\times$), and 50 ng/mL mouse epidermal growth factor (all from Life Technologies); and 1 mM N-acetylcysteine (Sigma—Aldrich) and mouse Noggin and mouse R-spondin-1, both as 10% conditioned medium. Medium was changed every 2 days. On day 2 after splitting, either 10 μM CFMB or 10 μM AR420626 was added to the medium. For control mouse organoids, regular medium without CFMB or AR420626 was used. Organoids were imaged on day 6, after 96 h of treatment, using a Nikon Inverted Spinning Disk confocal equipped with a humidified, temperature control environmental chamber. Images were obtained using NIS Elements AR software. To count the number of PYY positive cells in each organoid we obtained a continuous z-dimension stack (step size: 5 μM).

2.18. Wholemount immunostaining of organoids

Organoids were isolated from Matrigel, rinsed in PBS, and fixed in 4% PFA. After permeabilization for 30 min, organoids were blocked with 3% BSA. Organoids were incubated overnight with a primary antibody against GLP-1 (Abcam). Alexa Fluor 568 donkey anti-mouse (Jackson Laboratories) was used as secondary antibody. To count the number of GLP-1 positive cells in each organoid, we obtained a continuous z-dimension stack (step size: 5 μM) using a Nikon Inverted Spinning Disk confocal.

2.19. Statistics

Data are presented as the mean $\pm$ SEM. Most of the experiments were evaluated by a two-way ANOVA. A generalized estimating equation was applied for analysis of food intake and body weight. Comparisons were considered statistically significant when P was less than 0.05.

3. RESULTS

3.1. FFAR2 is required for the beneficial effects of fermentable carbohydrate supplementation on body weight

Inulin supplementation protects against body weight gain in humans and animals [10—12]. We hypothesized that this is due to FFAR2 activation by SCFAs following microbial fermentation. To investigate the contribution of FFAR2, $Ffar2^{-/-}$ mice and WT littermates were fed a HFD supplemented with inulin or a non-fermentable isocaloric control diet for 14 weeks. We have previously found that this diet results in a doubling of colonic SCFA concentration following 8 weeks supplementation in mice with the same genetic background [26].
Body weight was not affected by genotype at age 8—10 weeks when mice were fed standard chow (WT: 24.89 $\pm$ 0.34 g, $Ffar2^{-/-}$: 25.70 $\pm$ 0.42 g) (Supplementary Figure 1a). However, inulin supplementation exerted a protective effect against diet-induced obesity over the following 14 weeks, dependent on FFAR2 expression (percentage body weight change: WT HFC: 33.88 $\pm$ 2.83%, WT HFI: 20.38 $\pm$ 1.25%; $Ffar2^{-/-}$ HFC: 30.49 $\pm$ 2.38%, $Ffar2^{-/-}$ HFI: 30.67 $\pm$ 3.65%, p < 0.001) (Figure 1A). MRI analysis revealed that differences in body weight were due to decreased adiposity (p < 0.05) (Figure 1B). As expected, inulin supplementation also reduced liver triglyceride (p < 0.05) and leptin concentrations (p < 0.05) in WT mice, corresponding to lower fat mass (Figure 1C—D). Taken together, these data demonstrate that the ability of inulin to prevent weight gain in response to HFD is FFAR2-dependent.
The reduction in body weight observed in WT mice supplemented with inulin was associated with decreased food intake (WT HFC: 190.1 $\pm$ 5.9 g; WT HFI: 181.9 $\pm$ 5.7 g, $Ffar2^{-/-}$ HFC: 190.5 $\pm$ 3.7 g,

$Ffar2^{-/-}$ HFI: 193.6 $\pm$ 4.3 g (p < 0.05)) (Figure 1E). As appetite is regulated via appetite-inhibiting (anorexigenic) pro-opiomelanocortin (POMC) neurons and appetite-stimulating (orexigenic) neuropeptide Y (NPY) and agouti-related peptide (AgRP) co-expressing neurons within the hypothalamic arcuate nucleus, we measured gene expression of these neuropeptides. Expression of all three hypothalamic neuropeptides has previously been demonstrated to be sensitive to nutritional status, such that orexigenic neuropeptides Npy and $Agrp$ are elevated following fasting [36,37], while anorexigenic neuropeptide $Pomc$ expression is reduced [38]. As such gene expression of these neuropeptides serves as an indicator of anorectic drive. While we found that inulin supplementation did not alter $Pomc$ or Npy expression (Figure 1F—G), $Agrp$ expression was decreased in WT but not $Ffar2^{-/-}$ mice (p < 0.05) (Figure 1H), suggesting that inulin acts via FFAR2 to decrease hypothalamic orexigenic drive.
Body weight is not only a function of food intake, it is also governed by energy absorption and expenditure. To determine whether the reduction in body weight was associated with alterations in energy expenditure, we measured locomotor activity and basal metabolic rate, both of which were unaffected by diet or genotype (Figure 1I—J). As energy expenditure is influenced by brown adipose tissue thermogenesis, gene expression of the thermogenic protein $Ucp1$ was measured. In agreement with recently published data, gene expression of $Ucp1$ was unchanged following inulin supplementation (Figure 1K) [39]. To assess energy absorption, fecal energy content was measured. Inulin supplementation modestly reduced fecal energy loss in WT and $Ffar2^{-/-}$ mice (p < 0.05) (Figure 1L). Collectively, these data demonstrate the effect of inulin on body weight was not due to increased energy expenditure or fecal energy loss but was likely a result of the decrease in food intake.

3.2. Glucose homeostasis improvement following fermentable carbohydrate supplementation is dependent on FFAR2

Fermentable carbohydrate consumption has previously been shown to be associated with an improvement in glucose homeostasis [11]. Prior to dietary intervention, all groups were equally glucose tolerant and insulin sensitive (Supplementary Figure 2). After 13 weeks, WT mice given inulin exhibited improved glucose tolerance (p < 0.05). However, insulin tolerance was unchanged (Supplementary Figure 2). Interestingly, inulin lowered fasted glucose levels in WT and $Ffar2^{-/-}$ mice via a non-FFAR2 mediated mechanism (p < 0.01) (Supplementary Figure 2).

3.3. Deletion of FFAR2 does not alter the microbial density of *Bifidobacterium* spp., *Lactobacillus* spp., or total bacteria within the colon

Colonic microbial density and species composition influence inulin fermentation and SCFA production. Therefore, it was possible that FFAR2 could drive alterations in microbial diversity and account for the metabolic benefits we observed. To address this, we carried out targeted enquiry of bacterial species that are important for inulin fermentation and that are increased by fermentable carbohydrate supplementation. Total bacterial numbers were increased by inulin supplementation (p < 0.001), consistent with previous studies [40]. Additionally, species belonging to the *Bifidobacterium* spp., which play a key role in fermenting inulin, were also increased (p < 0.05), while the abundance of *Lactobacillus* spp. was unaltered. Importantly, there were no effects of genotype on microbial number or species-specific density (Figure 2); hence, the FFAR2-dependent effects of inulin on body weight are not driven by alterations in bacterial cell density.
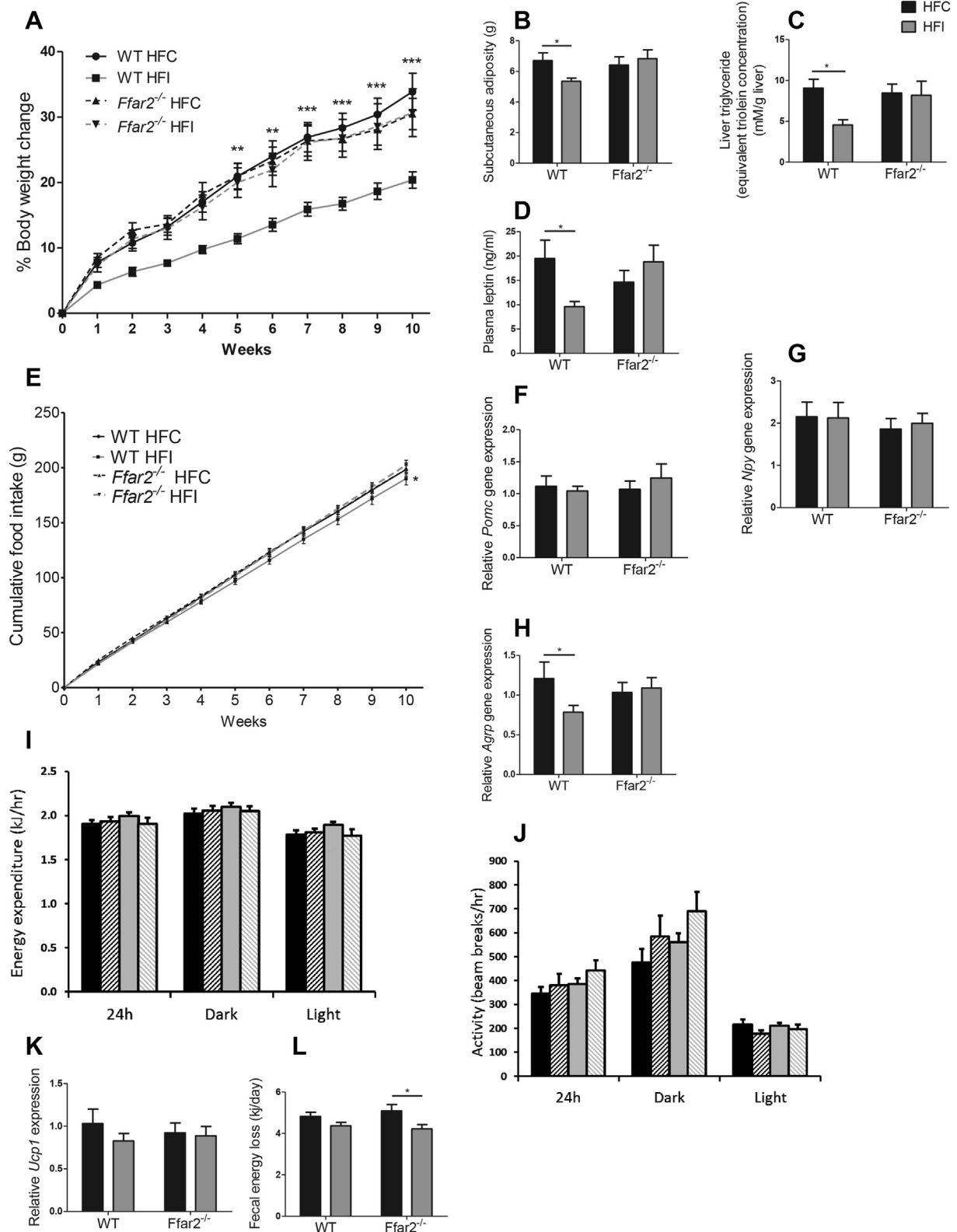
Figure 1: The effect of fermentable carbohydrate supplementation on metabolic parameters in high-fat fed WT and *Ffar2*$^{-/-}$ mice. Percentage body weight change (n = 19−22) (A), food intake (B), energy expenditure (C), activity (D), subcutaneous adiposity at 11 weeks (E), hepatic triglyceride (F), plasma leptin (G), fecal energy loss (H), hypothalamic expression of *Agrp* (I), *Npy* (J), *Pomc* (K), and scapular brown adipose tissue *Ucp1* expression (L) for male *Ffar2*$^{-/-}$ and WT littermate C57BL/6 mice fed a high-fat diet supplemented with inulin (HFI) or cellulose (HFC) (control) n = 10−12 over a 14 week period. Data represent mean ± S.E.M. *p < 0.05, **p < 0.01, ***p < 0.001. Statistical differences determined by GEE (A−B) or two-way ANOVA with post-hoc Bonferroni comparisons (C−H).
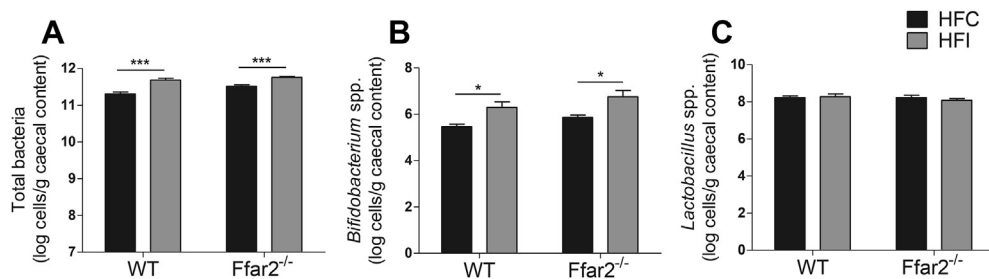
Figure 2: The effect of fermentable carbohydrate supplementation on bacterial density or species composition in high-fat fed WT and *Ffar2*$^{-/-}$ mice. Total bacteria (A), *Bifidobacteria spp.* (B), *Lactobacillus spp.* (C), for male *Ffar2*$^{-/-}$ and WT littermates fed a high-fat diet supplemented with inulin (HFI) or cellulose (HFC) (control) n = 10−12 over a 10 week period. Data represent mean ± S.E.M. *p < 0.05, ***p < 0.001. Statistical differences determined by two-way ANOVA with post-hoc Bonferroni comparisons.

3.4. Improvements in glucose homeostasis were not associated with adipose tissue immune cell infiltration

Obesity-associated inflammation impairs glucose homeostasis. As FFAR2 is involved in immune cell chemotaxis [41], we examined the white adipose tissue (WAT) immune cell phenotype (Supplementary Figure 3). FFAR2 deletion reduced the infiltration of subcutaneous WAT immune cells (CD45$^+$) and visceral WAT macrophages (CD11b$^+$ F4/80$^+$) as previously described [42] (p < 0.05). Inulin supplementation reduced CD4$^+$ T-cell infiltration in subcutaneous WAT of WT mice in association with improved glucose homeostasis (Supplementary Figure 2d) (p < 0.01). However, it is unlikely that reduced CD4$^+$ T-cell infiltration directly influenced glucose homeostasis as immune cell populations were also decreased by *Ffar2* deletion, which was not associated with such improvements. Conversely, one observation, which could account for improved glucose homeostasis, was that spontaneous TNF-α release from visceral WAT decreased following inulin supplementation in WT animals (p < 0.01) (Supplementary Figure 3j).

3.5. Improvements in glucose homeostasis were not associated with alterations in markers of intestinal barrier function

Systemic inflammation is also influenced by intestinal leakage of pro-inflammatory lipopolysaccharide (LPS). As microbiota influence intestinal barrier function [43], we measured gene expression of intestinal tight junction proteins as a marker of barrier integrity. Inulin supplementation caused a trend towards an increase in gene expression of tight junction proteins *ZO-1* and *Occludin* independently of genotype (Supplementary Figure 4a−c). Portal vein LPS was also measured as an indicator of barrier function. Inulin did not influence circulating LPS concentrations, indicating that alterations in intestinal barrier function are also unlikely to contribute to the observed metabolic improvements (Supplementary Figure 4d).

3.6. Fermentable carbohydrate supplementation stimulates FFAR2-dependent release of PYY

Increased PYY and GLP-1 secretion has been implicated in mediating the effects of fermentable carbohydrate on body composition and glucose homeostasis [44,45]. To investigate whether changes in body weight were associated with release of these hormones, we measured portal vein PYY and GLP-1 concentrations following 2 weeks dietary intervention before significant differences in body weight between groups are apparent. Inulin supplementation significantly increased circulating PYY in WT (p < 0.05) but not in *Ffar2*$^{-/-}$ mice (p = 0.39) (WT HFC: 54.7 ± 17.0 pmol L^{-1}, WT HFI: 84.9 ± 19.3 pmol L^{-1}, *Ffar2*$^{-/-}$ HFC: 52.8 ± 22.2 pmol L^{-1}, *Ffar2*$^{-/-}$ HFI: 66.91 ± 28.4 pmol L^{-1}) (Figure 3A). The ability of inulin to increase

portal vein PYY appears to be reduced and not completely abolished by FFAR2 deletion, as the difference between WT HFI and *Ffar2*$^{-/-}$ HFI groups was not significant. In contrast to PYY, GLP-1 release was increased independently of FFAR2 following inulin supplementation (WT: p < 0.05, *Ffar2*$^{-/-}$: 0.0548) (Figure 3B), demonstrating that inulin differentially regulates PYY and GLP-1 secretion via FFAR2-dependent and independent mechanisms respectively.

While SCFAs are implicated in mediating the effects of inulin due to the selectivity of FFAR2 for these metabolites, we confirmed their role in a primary colonic cell model [31]. Exposure to mixed SCFAs, in the same ratio as found in the gut following inulin fermentation [46], increased secretion of PYY by 127% (p < 0.0001) and GLP-1 by 54% (p < 0.001) compared to baseline. This effect was not observed in *Ffar2*$^{-/-}$ tissue (PYY: p = 0.07, GLP-1: p = 0.42), indicating SCFAs act via FFAR2 to stimulate both PYY and GLP-1 secretion (Figure 3C−D). These findings are similar to the results of Tolhurst et al., who demonstrated FFAR2-dependent GLP-1 release in response to mixed SCFAs [24]. The dependence of SCFA-induced GLP-1 secretion on FFAR2 expression is contrary to the receptor-independent effects observed *in vivo*. This may be due to SCFAs acting via different acute vs. chronic mechanisms. Alternatively, other fermentation products present *in vivo* could influence GLP-1 secretion.

3.7. Fermentable carbohydrate acts via FFAR2 to specifically increase colonic PYY

Increased concentrations of circulating PYY and GLP-1 following inulin supplementation may reflect an increased capacity of the gut to secrete these hormones due to increased colonic hormone content. To address this, we measured colonic PYY and GLP-1 concentrations. Following inulin supplementation, colonic PYY was increased by 130%, (p < 0.05) an effect that was abolished in *Ffar2*$^{-/-}$ animals (p = 0.65) (Figure 3E). In contrast, inulin significantly increased colonic GLP-1 regardless of genotype and thus was not receptor dependent (WT: p < 0.01, *Ffar2*$^{-/-}$: p < 0.01) (Figure 3F). These effects were specific to L cells as hormones expressed in developmentally distinct enteroendocrine cell types such as GIP and Substance P were unchanged. Crypt length as well as goblet and enterochromaffin cell densities were also unaffected (Supplementary Figure 5). Colonic PYY and GLP-1 concentrations reflected the circulating concentrations, indicating that inulin increases gut hormone release by increasing the amount of PYY and GLP-1 within the colon.

3.8. Fermentable carbohydrate supplementation increases PYY cell density in the proximal colon via FFAR2

To determine whether the increased colonic PYY and GLP-1 concentrations were due to an increase in L cell density, we used
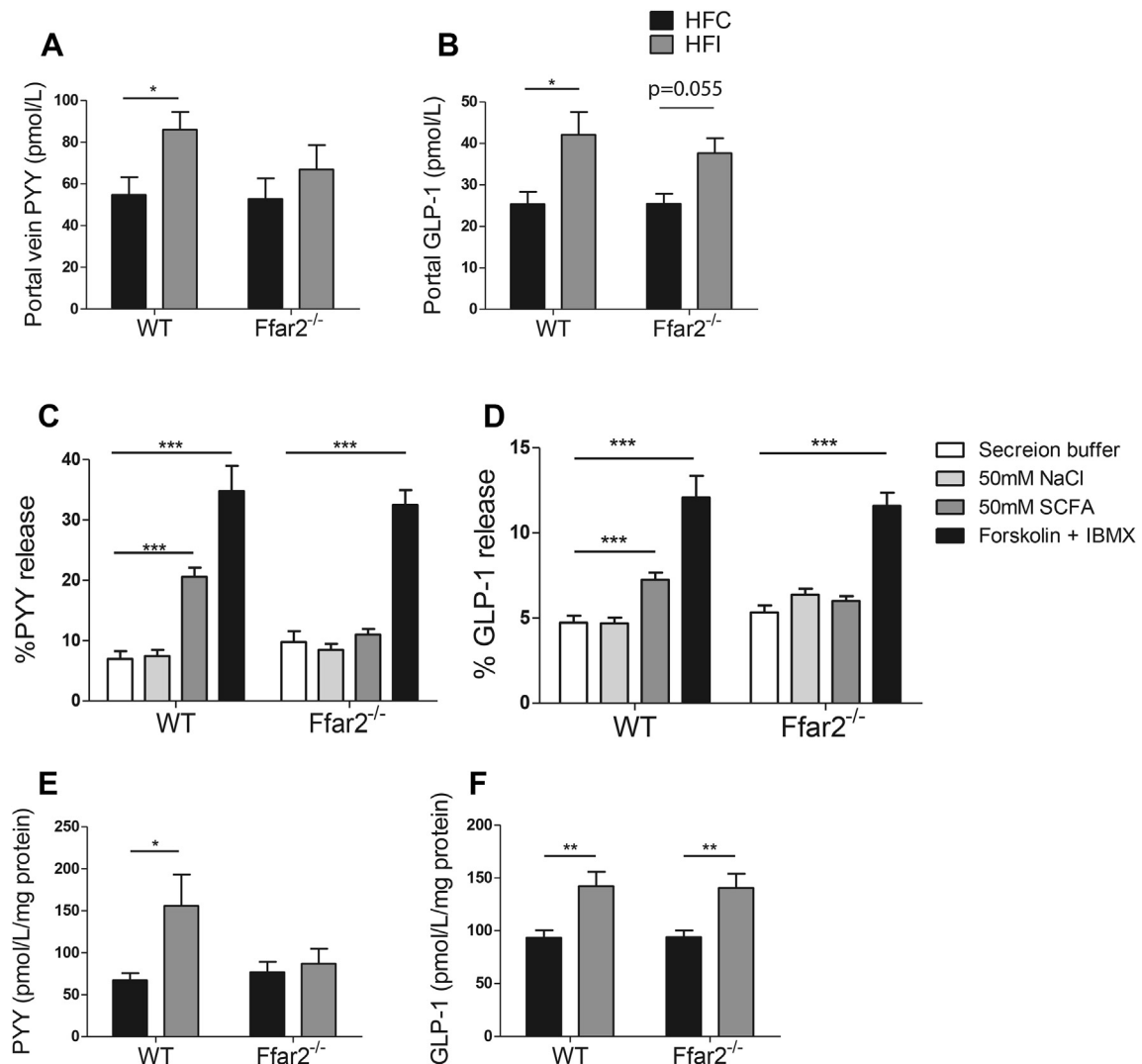
Figure 3: Gut hormone concentration following fermentable carbohydrate supplementation or incubation with SCFA in WT and *Ffar2*$^{-/-}$ mice. Portal vein peptide YY (PYY) (A), portal vein Glucagon-like peptide-1 (GLP-1) (B), colonic PYY (C), and colonic GLP-1 (D) concentrations of male *Ffar2*$^{-/-}$ and WT littermates fed a high-fat diet supplemented with inulin (HFI) or cellulose (HFC) for 14 weeks (A—B, n = 10—12) or 2 weeks (C—D n = 4—6). Percentage PYY (E) of GLP-1 (F) release from mixed colonic cultures taken from *Ffar2*$^{-/-}$ and WT littermates controls following incubation with 50 mM SCFA (30 mM acetate, 12.5 mM propionate, 7.5 mM butyrate) (E). Data represent mean ± S.E.M. *p < 0.05, **p < 0.01, ***p < 0.001. Statistical differences determined by student's t-test or two-way ANOVA with post-hoc Bonferroni comparisons.

immunofluorescent staining to quantify PYY- and GLP-1-expressing cells. Body weight at the time of tissue collection was not significantly different between groups (2 weeks on inulin supplemented diet) (Supplementary Figure 6). In WT mice, inulin supplementation caused an 87% increase in PYY (p < 0.05) and 73% increase in GLP-1 cell density (p < 0.05). Whereas, in *Ffar2*$^{-/-}$ mice, GLP-1 cell density was increased by 60% (p < 0.05), and PYY cell-density was unchanged (p = 0.23) (Figure 4). While the expansion of the PYY-expressing cell population is dependent on FFAR2, the expansion of the GLP-1-expressing cell population occurs independently of FFAR2. We also observed an increase in the density of cells that co-express both hormones (Figure 4C). Therefore, the increase in GLP-1 cell density appears to be due to GLP-1 being expressed in cells that would otherwise have been PYY singly labeled cells. Conversely, the increase in PYY cell density was due to an expansion of L cells that did not express GLP-1. These data demonstrate that inulin increases colonic gut hormone concentrations by increasing the density of specific enteroendocrine cell types in the colon.

To assess whether increased PYY cell density was due to an increase in the rate of PYY cell formation, bromodeoxyuridine (BrdU) was administered to mice for the second week of a 2-week intervention. BrdU incorporates into the DNA of dividing cells, allowing identification of newly formed cells. PYY-expressing cells, which stained positive for BrdU, were 129% more abundant in WT (p = 0.0003) but not *Ffar2*$^{-/-}$ mice (p = 0.53) following inulin supplementation (Figure 4D), confirming that inulin promotes formation of new PYY cells in a FFAR2-dependent manner.

In rodents, the intestinal epithelium is replaced every 4—5 days [47]. Newly formed colonic cells are generated from multipotent stem cells through progressive restrictions in developmental potential. The fate of a cell is the result of the expression of specific transcription factors, which orchestrate intricate differentiation pathways by regulating the transcription of various genes. While it is currently unclear which factors direct expression of each specific gut hormone, transcription factors known to function in terminal differentiation of GLP-1 and PYY cells include *Pax4*, *Pax6*, *Foxa1*, and *Foxa2* [48—51]. To further
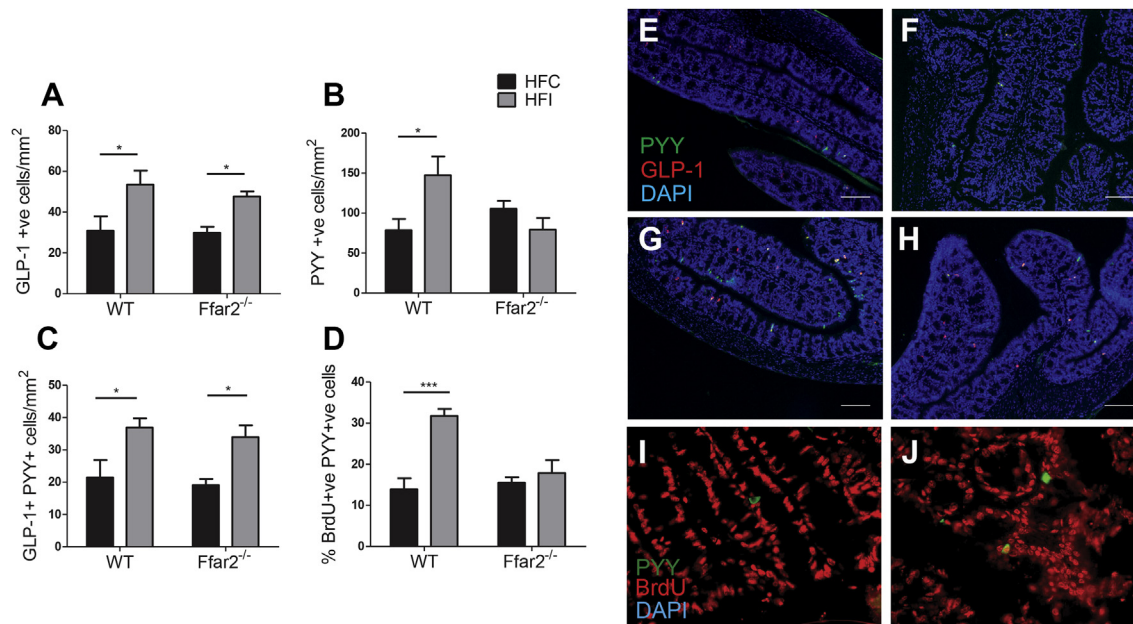
Figure 4: The effect of fermentable carbohydrate supplementation on L cell density in high-fat fed WT and _Ffar2_$^{-/-}$ mice. PYY (A), GLP-1 (B), GLP-1/PYY co-localized cells per mm^2 (C) and the percentage of PYY+ cells which also stained positive for BrdU (D) within the proximal colon of male _Ffar2_$^{-/-}$ and WT littermates fed a high-fat diet supplemented with inulin (HFI) or cellulose (HFC) for 2 weeks (n = 4—6). Representative images of PYY and GLP-1 staining are shown in E, F, G, and H. Representative images of PYY and BrdU staining are shown in I and J. Scale bars are equal to 100 μm. Data represent mean ± S.E.M. *p < 0.05, ***p < 0.001. Statistical differences determined by two-way ANOVA with post-hoc Bonferroni comparisons.

elucidate the mechanism by which inulin regulates the expansion of PYY cells, we measured gene expression of these transcription factors. While _Pax6_, _Foxa1_ and _Foxa2_ were unaltered following inulin feeding, _Pax4_ was significantly and receptor-dependently increased (WT: p = 0.017, _Ffar2_$^{-/-}$: p = 0.69) (Figure 5). This suggests that _Pax4_ may link FFAR2 activation to the expansion of the PYY cell population.

3.9. FFAR2 but not FFAR3 activation increases PYY cell density _in vitro_

To determine the relative roles of FFAR2 and FFAR3 on PYY and GLP-1 cell density, we used selective agonists for FFAR2 (CFMB) [52] and FFAR3 (AR420626) [35] in an _in vitro_ organoid culture. The doses of each agonist were chosen based on previous reports in the literature and because they did not result in cellular toxicity in our organoid model. Tolhurst et al. demonstrate that a dose of 30 μM of CFMB increases calcium flux in isolated colonic cultures [45]. Whilst Nohr et al. [46] used doses of 10 μM and 30 μM of both agonists based on their potencies. CFMB is reported to have an IC$_{50}$ of 4.7 μM at FFAR2 but displays no activity at FFAR3 up to 1 mM, while AR420626 is reported to have an IC$_{50}$ value of 117 nM for FFAR3 and does not activate FFAR2 at concentrations up to 100 μM in cAMP accumulation assays [52]. Primary intestinal crypts from PYY-GFP mice were cultured in a three-dimensional, growth-factor rich environment, recapitulating _in vivo_ colonic multi-lineage differentiation [35,53]. Exposure of colonic organoids to FFAR2 agonist CFMB led to increased PYY, but not GLP-1 cell density (p < 0.001) (Figure 6). In contrast, the FFAR3 agonist had no effect on PYY or GLP-1 cell density. It therefore appears that SCFAs act via FFAR2 but not FFAR3 to increase PYY cell density.

4. DISCUSSION

The discovery that gut microbiota influences physiology and, in certain circumstances, may cause disease pathologies has led to an intensive research effort to unravel microbiota—host interactions. Understanding the effects of microbial fermentation on host metabolism has been of particular interest, because consumption of fermentable carbohydrate reduces appetite and prevents body weight gain [10—12,20]. Evidence points to the production of SCFAs by the gut microbiota as an important appetite regulatory signal. In this study, we report for the first time that FFAR2 expression is essential for inulin to exert these beneficial effects. As such, targeting this pathway in man could be a viable means of preventing obesity.

Our key finding is that fermentable carbohydrate drives an increase in PYY-cell density within the colon, which is mediated via FFAR2 and results in increased circulating PYY concentrations. This is associated with a reduction in food intake and protection against diet-induced obesity. Furthermore, FFAR2 but not FFAR3 activation at the level of the intestinal epithelium is sufficient to increase PYY cell density in isolated organoids. We also demonstrate that inulin, acting via FFAR2, stimulates the expression of _Pax4_, a transcription factor that has previously been shown to be essential for differentiation of PYY cells in the fetal mouse colon [54]. We therefore propose that inulin, following microbial fermentation to SCFAs, acts via FFAR2 to influence cellular differentiation pathways and promote PYY cell fate. Increasing the density of PYY cells provides the colon with a greater potential for release of PYY, which is known to reduce food intake.

A number of interesting questions remain to be answered. As FFAR2 activation drives changes in enteroendocrine cell fate, is it expressed by progenitor cells, either by epithelial LgR5+ stem cells or by endocrine NGN3+ progenitors, or does FFAR2 act later in the enteroendocrine development pathway? Lineage tracing experiments could allow the determination of the origin of newly generated PYY singly labeled cells. Furthermore, it will be important in the future to determine the intracellular pathways triggered by FFAR2 activation that lead to altered endocrine cell fate. Understanding these processes could identify targets for manipulation of endocrine cell fate in order to treat disease.
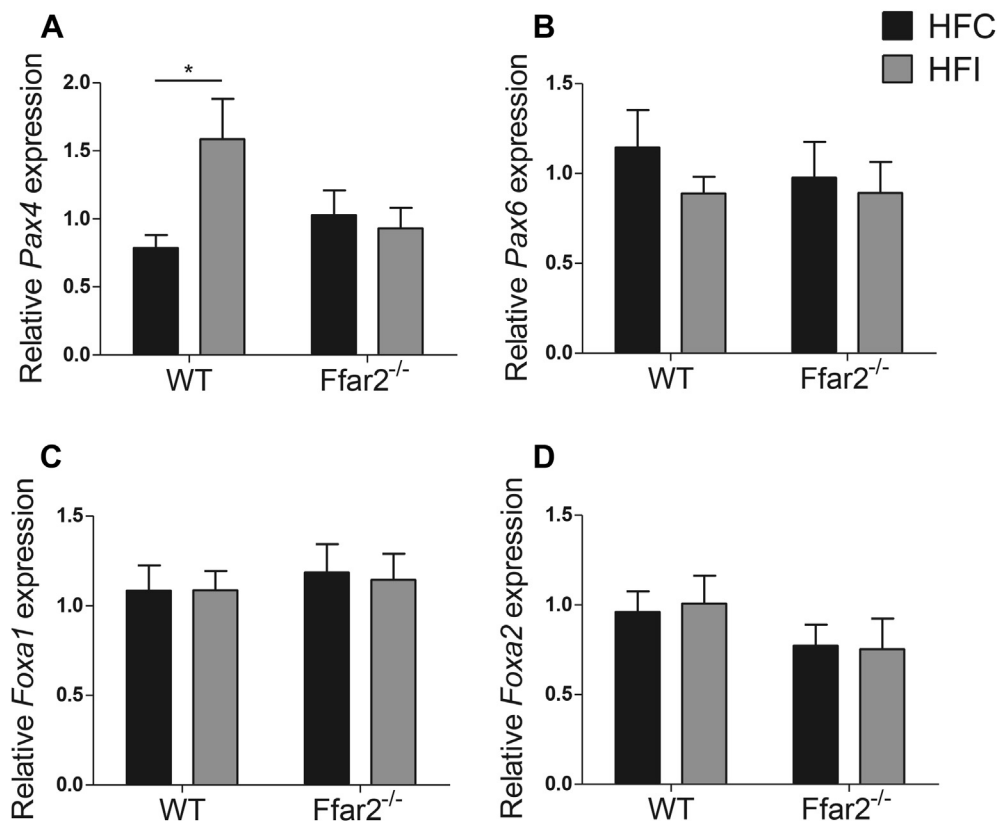
Figure 5: The effect of fermentable carbohydrate on colonic transcription factor expression *in vivo*. Gene expression relative to 18S was determined for *Pax4* (A) *Pax6* (B), *Foxa1* (C), and *Foxa2* (D) in the colon of male *Ffar2*$^{-/-}$ and WT littermates fed a high-fat diet supplemented with inulin (HFI) or cellulose (HFC) for 2 weeks, n = 6–8. Data represent mean ± S.E.M. *p < 0.05. Statistical differences determined by two-way ANOVA with post-hoc Bonferroni comparisons.

While we describe an important role for FFAR2 in driving increased PYY secretion, FFAR2 signaling has previously been reported to influence food intake and body weight via the inhibition of ghrelin secretion [52] and the suppression of insulin signaling in adipocytes [55]. As such, it is likely that SCFAs exert their effects on metabolism via multiple complementary pathways. However, fermentation occurs primarily in the colon where there is a high density of L cells, suggesting that the mechanism described here plays a critical role in transducing the effects of SCFAs on appetite.

The luminal concentrations of SCFAs within the colon have been estimated to be 70–130 mmol [56]. This exceeds the concentration range to which FFAR2 is sensitive and would suggest that colonic FFAR2 is constantly active. However, due to a number of factors, it is unlikely that FFA receptors are exposed to these concentrations. Firstly, in the colon, the microbiota are compartmentalized to the outer mucus layer; the inner mucus layer contains almost no microbiota and serves to protect the epithelium. Therefore, there is a separation between the bacteria and the epithelium, through which a concentration gradient would form. In the distal colon, the ~50 μm inner mucus layer has been shown to be replaced every hour [57]. Secondly, the crypt opening is narrow, creating further impediment to the diffusion of SCFAs. Finally, SCFAs are rapidly absorbed by the epithelial cells, thereby depleting the concentration of SCFAs in the immediate environment. The precise concentration of the different SCFAs at the level of the colonic epithelium is not known. However, based on the EC$_{50}$ values of SCFAs for FFAR2 one might imagine that the local SCFA concentration would be in the micromolar range [15].

Additionally, there are likely to be non-receptor mediated actions of SCFAs following dietary fermentable carbohydrate supplementation. Recently, it has been demonstrated that acetate alters hypothalamic neuronal activity [58]. However, the central actions of SCFAs on food intake, to date, have only been observed acutely following intra-cerebroventricular administration [58]. In contrast, our data describe long-term FFAR2-dependent adaptations, which may underlie the ability of fermentable carbohydrates to exert sustained reductions in body weight. SCFA also have been reported to act via a non-receptor mediated mechanism within the liver and adipose tissue to reduce peroxisome proliferator-activated receptor gamma (PPAR-γ) expression, thereby preventing body weight gain and improving insulin sensitivity [59]. These observations are described following dietary supplementation with SCFAs as opposed to fermentable carbohydrate. In contrast to the microbiota-dependant production of SCFAs from fermentable carbohydrate, dietary SCFAs can be absorbed earlier in the gastrointestinal tract, and therefore colonic mechanisms would be largely evaded. Collectively, the accumulating data within this field reveal a complex system of intertwined receptor- and non-receptor mediated mechanisms that act together to prevent body weight gain. In agreement with previous studies, we also find that fermentable carbohydrate increased GLP-1 secretion [44,45]. This could explain the decreased fasted plasma glucose observed with inulin supplementation due to the insulinotropic effects of GLP-1 [60]. In support of this, it has recently been demonstrated that dibenzazepine administration, which blocks the Notch signaling pathway, increases intestinal GLP-1 cell numbers in a HFD model of impaired glucose tolerance and
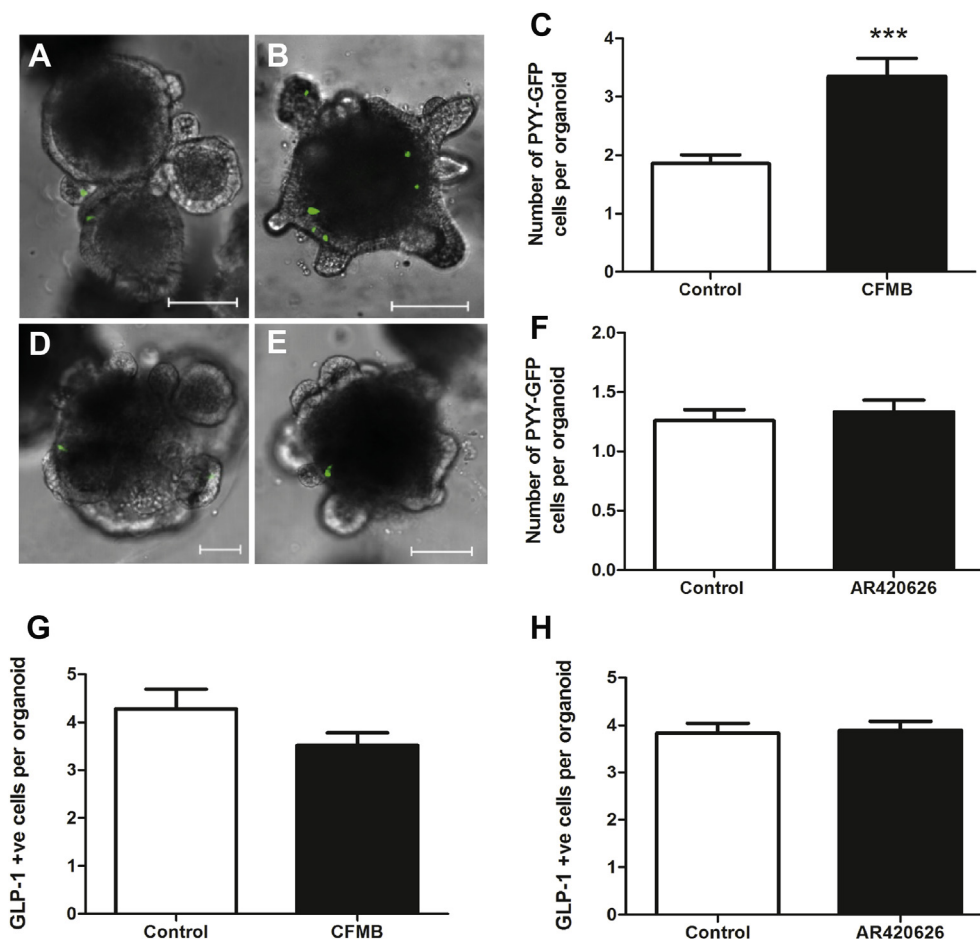
Figure 6: Effect of CFMB and AR420626 on PYY and GLP-1 cell fate in intestinal organoids. Organoids from PYY-GFP mice were cultured in absence (A, D) or presence of 10 μM CFMB (B) and 10 μM AR420626 (E) for 96 h. Shown are Z-stack projections covering the whole organoid. Scale bars: 100 μm. (C, F) PYY cell numbers after 96 h continuous exposure with 10 μM CFMB (C) and 10 μM AR420626 (F). n = 30−60 organoids (2 platings). Number of GLP-1 +ve cells in organoids from PYY-GFP mice after 96-hour exposure to CFMB (G) and AR420626 (H). n = 100−300 organoids (3 platings). Expression of *Pyy* (I) and *Gcg* (J) following 96-hour exposure to CFMB in WT and *Ffar2*$^{-/-}$ organoids. All data are presented as mean ± S.E.M, ****$p < 0.0001$, ***$p < 0.001$. *$p < 0.05$. Statistical differences determined by nonpaired 2-tailed Student's t test (C, F, G, H) or 2-way ANOVA (I−J).

improves insulin responses to glucose and glucose tolerance [61]. Alternatively, recently published data suggest that the improvements in glucose homeostasis could be associated with FFAR3-dependant alterations in intestinal gluconeogenesis [62,63]. Propionate signals via FFAR3 expressed on periportal afferent neurons and via a gut-brain neural circuit to induce intestinal gluconeogenesis, which results in improved glucose homeostasis [63].

Similar to the increase in PYY, the increase in circulating GLP-1 was associated with a greater cell density. Previously Cani et al. have demonstrated that fermentable carbohydrate increases colonic GLP-1 cell density in association with increased expression of the transcription factor Neurogenin3 (NGN3) [44,64]. NGN3 acts upstream of Pax4, Pax6, Foxa1, and Foxa2 and is responsible for determining an enteroendocrine cell fate. This suggests that fermentable carbohydrate increases production of new enteroendocrine cells. However, the observed increase in GLP-1 cell density was not associated with alterations in *Pax4*, *Pax6*, *Foxa1*, and *Foxa2* expression, indicating that these transcription factors are not responsible for driving increases in GLP-1 cell density in response to inulin.

Contrary to the increase in PYY cell density, the increase in GLP-1 cell density occurred independently of FFAR2. In agreement with a number of other studies, we found only partial co-localization of PYY and GLP-1 [23,65−69], despite the prevailing view that GLP-1 and PYY are co-expressed in L cells and co-stored in secretory vesicles. This may be because the degree of co-localization varies depending on location along the proximal−distal axis, between species, with metabolic state, and between studies [66,67]. It is therefore of great interest to identify factors that differentially modulate the expression of these two gut hormones.

The mechanism underlying the increase in GLP-1 cell density does not appear to be FFAR3 activation, as FFAR3 agonism did not alter the density of GLP-1 cells in organoids. Furthermore, *Ffar2* deletion has previously been shown to prevent SCFA-induced GLP-1 release *in vitro* to a greater degree than FFAR3 deletion [24], suggesting that FFAR3 may be less important in mediating SCFA signaling in L cells. One possibility is that SCFAs cross the cell membrane via non-ionic diffusion and may act intracellularly to increase GLP-1 cell density [70]. However, such a mechanism perhaps would be associated with a more generalized proliferative effect compared to the very specific effects that we observed. Finally, and more plausibly, additional bioactive fermentation products may stimulate an expansion of the GLP-1 cell population. Undoubtedly, elucidation of this mechanism will
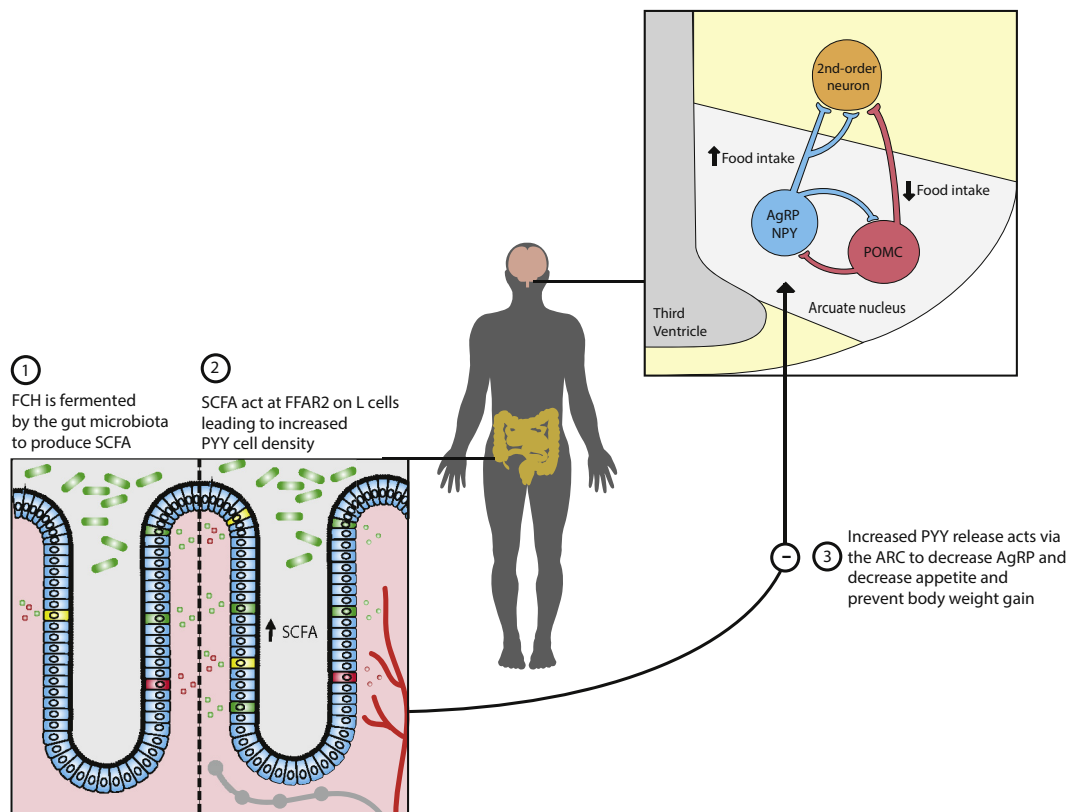
Figure 7: Mechanism by which fermentable carbohydrate prevents body weight gain. Following consumption, fermentable carbohydrate (FCH) is fermented by gut microbiota to produce short chain fatty acids (SCFAs). SCFAs subsequently act at free fatty acid receptor 2 (FFAR2) within the colon to enhance PYY cell density, thereby augmenting the capacity of the gut to release PYY. PYY acts to reduce orexigenic drive via AgRP neurons within the arcuate nucleus and reduce food intake.

be an important discovery that could improve treatment options for diabetes.

5. CONCLUSION

We have demonstrated that FFAR2 is pivotal for transducing the beneficial metabolic effects of fermentable carbohydrate. By stimulating microbial SCFA production using inulin, we demonstrate that these fermentation products act via FFAR2 to drive an expansion of the PYY cell population within the proximal colon. The resulting increase in cell density leads to increased circulating PYY, which previously has been shown to reduce appetite [71]. This presents a new understanding of gut physiology whereby the gut exhibits cellular plasticity, allowing it to respond to alterations in dietary composition. Such changes alter the capacity for anorectic signaling (Figure 7). This paradigm likely represents a more general physiological mechanism and, if true, begs the question as to whether other nutrients or microbial metabolites influence enteroendocrine plasticity in order to alter host physiology. By targeting this pathway with drugs or nutraceuticals, it may be possible to prime the colon to produce a greater anorectic signal in response to nutrients to treat or prevent obesity.

AUTHOR CONTRIBUTIONS

CONFLICT OF INTEREST

None declared.

APPENDIX A. SUPPLEMENTARY DATA

Supplementary data related to this article can be found at http://dx.doi.org/10.1016/j.molmet.2016.10.011.

REFERENCES

[1] Calle, E.E., Kaaks, R., 2004. Overweight, obesity and cancer: epidemiological evidence and proposed mechanisms. Nature Reviews Cancer 4(8):579—591.

[2] Hajer, G.R., van Haeften, T.W., Visseren, F.L.J., 2008. Adipose tissue dysfunction in obesity, diabetes, and vascular diseases. European Heart Journal 29(24):2959—2971.

[3] Luc, F.V.G., Ilse, L.M., Christophe, E.D.B., 2006. Mechanisms linking obesity with cardiovascular disease. Nature 444(7121):875—880.

[4] Bäckhed, F., et al., 2004. The gut microbiota as an environmental factor that regulates fat storage. Proceedings of the National Academy of Sciences of the United States of America 101(44):15718—15723.

[5] Ley, R.E., et al., 2005. Obesity alters gut microbial ecology. Proceedings of the National Academy of Sciences of the United States of America 102(31):11070—11075.

[6] Ley, R.E., et al., 2006. Microbial ecology: human gut microbes associated with obesity. Nature 444(7122):1022—1023.

[7] Turnbaugh, P.J., et al., 2006. An obesity-associated gut microbiome with increased capacity for energy harvest. Nature 444(7122):1027—1031.

[8] Macfarlane, G.T., Gibson, G.R., 1995. Microbiological aspects of production of short-chain fatty acids in the large bowel. In: Rombeau, J., Cummings, J.H., Sakata, T. (Eds.), Physiological and clinical aspects of short-chain fatty acids. Cambridge: Cambridge University Press. p. 87—105.

[9] Sleeth, M.L., et al., 2010. Free fatty acid receptor 2 and nutrient sensing: a proposed role for fibre, fermentable carbohydrates and short-chain fatty acids in appetite regulation. Nutrition Research Reviews 23(1):135—145.

[10] So, P.W., et al., 2007. Impact of resistant starch on body fat patterning and central appetite regulation. PLoS One 2(12):e1309.

[11] Cani, P.D., et al., 2006. Improvement of glucose tolerance and hepatic insulin sensitivity by oligofructose requires a functional glucagon-like peptide 1 receptor. Diabetes 55(5):1484—1490.

[12] Parnell, J.A., Reimer, R.A., 2009. Weight loss during oligofructose supplementation is associated with decreased ghrelin and increased peptide YY in overweight and obese adults. American Journal of Clinical Nutrition 89(6):1751—1759.

[13] Liou, A.P., et al., 2013. Conserved shifts in the gut microbiota due to gastric bypass reduce host weight and adiposity. Science Translational Medicine 5(178), p. 178ra41-178ra41.

[14] Wolever, T.M., et al., 1989. Effect of rectal infusion of short chain fatty acids in human subjects. The American Journal of Gastroenterology 84(9):1027—1033.

[15] Brown, A.J., et al., 2003. The Orphan G protein-coupled receptors GPR41 and GPR43 are activated by propionate and other short chain carboxylic acids. Journal of Biological Chemistry 278(13):11312—11319.

[16] Le Poul, E., et al., 2003. Functional characterization of human receptors for short chain fatty acids and their role in polymorphonuclear cell activation. Journal of Biological Chemistry 278(28):25481—25489.

[17] Karaki, S., et al., 2006. Short-chain fatty acid receptor, GPR43, is expressed by enteroendocrine cells and mucosal mast cells in rat intestine. Cell and Tissue Research 324(3):353—360.

[18] Karaki, S., et al., 2008. Expression of the short-chain fatty acid receptor, GPR43, in the human colon. Journal of Molecular Histology 39(2):135—142.

[19] Tazoe, H., et al., 2009. Expression of short-chain fatty acid receptor GPR41 in the human colon. Biomedical Research 30(3):149—156.

[20] Frost, G., et al., 2014. The short-chain fatty acid acetate reduces appetite via a central homeostatic mechanism. Nature Communications 5:3611.

[21] Engelstoft, M.S., et al., 2008. A gut feeling for obesity: 7TM sensors on enteroendocrine cells. Cell Metabolism 8(6):447—449.

[22] Cummings, D.E., Overduin, J., 2007. Gastrointestinal regulation of food intake. Journal of Clinical Investigation 117(1):13—23.

[23] Eissele, R., et al., 1992. Glucagon-like peptide-1 cells in the gastrointestinal tract and pancreas of rat, pig and man. European Journal of Clinical Investigation 22(4):283—291.

[24] Tolhurst, G., et al., 2012. Short-chain fatty acids stimulate glucagon-like peptide-1 secretion via the G-protein—coupled receptor FFAR2. Diabetes 61(2):364—371.

[25] Maslowski, K.M., et al., 2009. Regulation of inflammatory responses by gut microbiota and chemoattractant receptor GPR43. Nature 461(7268):1282—1286.

[26] Anastasovska, J., et al., 2012. Fermentable carbohydrate alters hypothalamic neuronal activity and protects against the obesogenic environment. Obesity 20(5):1016—1023.

[27] Melgar, S., et al., 2007. Mice with experimental colitis show an altered metabolism with decreased metabolic rate. American Journal of Physiology. Gastrointestinal and Liver Physiology 292(1):G165—G172.

[28] Everard, A., et al., 2013. Cross-talk between *Akkermansia muciniphila* and intestinal epithelium controls diet-induced obesity. Proceedings of the National Academy of Sciences of the United States of America 110(22):9066—9071.

[29] Stolarczyk, E., et al., 2013. Improved insulin sensitivity despite increased visceral adiposity in mice deficient for the immune cell transcription factor T-bet. Cell Metabolism 17(4):520—533.

[30] Sam, A.H., et al., 2012. Selective ablation of peptide YY cells in adult mice reveals their role in beta cell survival. Gastroenterology 143(2):459—468.

[31] Reimann, F., et al., 2008. Glucose sensing in L cells: a primary cell study. Cell Metabolism 8(6):532—539.

[32] Adrian, T.E., et al., 1985. Human distribution and release of a putative new gut hormone, peptide YY. Gastroenterology 89(5):1070—1077.

[33] Kreymann, B., et al., 1987. Glucagon-like peptide-1 7-36: a physiological incretin in man. Lancet 2(8571):1300—1304.

[34] Bohorquez, D.V., et al., 2011. Characterization of basal pseudopod-like processes in ileal and colonic PYY cells. Journal of Molecular Histology 42(1):3—13.

[35] Sato T, et al. Single Lgr5 stem cells build crypt-villus structures in vitro without a mesenchymal niche. (1476—4687 (Electronic)).

[36] Hahn, T.M., et al., 1998. Coexpression of Agrp and NPY in fasting-activated hypothalamic neurons. Nature Neuroscience 1(4):271—272.

[37] White, J.D., Kershaw, M., 1990. Increased hypothalamic neuropeptide Y expression following food deprivation. Molecular and Cellular Neuroscience 1(1):41—48.

[38] Mizuno, T.M., et al., 1998. Hypothalamic pro-opiomelanocortin mRNA is reduced by fasting and [corrected] in ob/ob and db/db mice, but is stimulated by leptin. Diabetes 47(2):294—297.

[39] Alligier, M., et al., 2014. Positive interaction between prebiotic nutrients and thiazolidinedione treatment on adiposity in diet-induced obese mice. Obesity.

[40] Campbell, J.M., Fahey, G.C., Wolf, B.W., 1997. Selected indigestible oligosaccharides affect large bowel mass, cecal and fecal short-chain fatty acids, pH and microflora in rats. The Journal of Nutrition 127(1):130—136.

[41] Vinolo, M.A.R., et al., 2011. SCFAs induce mouse neutrophil chemotaxis through the GPR43 receptor. PLoS One 6(6):e21205.

[42] Bjursell, M., et al., 2011. Improved glucose control and reduced body fat mass in free fatty acid receptor 2-deficient mice fed a high-fat diet. American Journal of Physiology. Endocrinology and Metabolism 300(1):E211—E220.

[43] Cani, P.D., et al., 2007. Metabolic endotoxemia initiates obesity and insulin resistance. Diabetes 56(7):1761—1772.

[44] Cani, P.D., et al., 2007. Dietary non-digestible carbohydrates promote L-cell differentiation in the proximal colon of rats. British Journal of Nutrition 98(01): 32—37.

[45] Verhoef, S.P., Meyer, D., Westerterp, K.R., 2011. Effects of oligofructose on appetite profile, glucagon-like peptide 1 and peptide YY3-36 concentrations and energy intake. British Journal of Nutrition 106(11):1757—1762.

[46] McNeil, N.I., 1984. The contribution of the large intestine to energy supplies in man. The American Journal of Clinical Nutrition 39(2):338—342.

[47] van der Flier, L.G., Clevers, H., 2009. Stem cells, self-renewal, and differentiation in the intestinal epithelium. Annual Review of Physiology 71(1): 241—260.

[48] Ye, D.Z., Kaestner, K.H., 2009. Foxa1 and Foxa2 control the differentiation of goblet and enteroendocrine L- and D-cells in mice. Gastroenterology 137(6): 2052—2062.

[49] Beucher, A., et al., 2012. The homeodomain-containing transcription factors Arx and Pax4 control enteroendocrine subtype specification in mice. PLoS One 7(5):e36449.

[50] Larsson, L.-I., et al., 1998. Pax 4 and 6 regulate gastrointestinal endocrine cell development. Mechanisms of Development 79(1—2):153—159.

[51] Schonhoff, S.E., Giel-Moloney, M., Leiter, A.B., 2004. Minireview: development and differentiation of gut endocrine cells. Endocrinology 145(6):2639—2644.

[52] Engelstoft, M.S., et al., 2013. Seven transmembrane G protein-coupled receptor repertoire of gastric ghrelin cells. Molecular Metabolism 2(4):376—392.

[53] Sato T, Clevers H. Growing self-organizing mini-guts from a single intestinal stem cell: mechanism and applications. (1095—9203 (Electronic)).

[54] Udupi, V., et al., 1998. Pax4 is required for differentiation of peptide YY (PYY) cells in mouse colon. Gastroenterology 114:A912.

[55] Kimura, I., et al., 2013. The gut microbiota suppresses insulin-mediated fat accumulation via the short-chain fatty acid receptor GPR43. Nature Communications 4:1829.

[56] Mortensen, P.B., Clausen, M.R., 1996. Short-chain fatty acids in the human colon: relation to gastrointestinal health and disease. Scandinavian Journal of Gastroenterology Supplement 216:132—148.

[57] Johansson, M.E., 2012. Fast renewal of the distal colonic mucus layers by the surface goblet cells as measured by in vivo labeling of mucin glycoproteins. PLoS One 7(7):e41009.

[58] Frost, G., et al., 2014. The short-chain fatty acid acetate reduces appetite via a central homeostatic mechanism. Nature Communications 5.

[59] den Besten, G., et al., 2015. Short-chain fatty acids protect against high-fat diet-induced obesity via a PPARgamma-dependent switch from lipogenesis to fat oxidation. Diabetes.

[60] Parkes, D.G., et al., 2001. Insulinotropic actions of exendin-4 and glucagon-like peptide-1 in vivo and in vitro. Metabolism 50(5):583—589.

[61] Petersen, N., et al., 2015. Targeting development of incretin-producing cells increases insulin secretion. The Journal of Clinical Investigation 125(1):379—385.

[62] De Vadder, F., et al., 2014. Microbiota-generated metabolites promote metabolic benefits via gut-brain neural circuits. Cell 156(1):84—96.

[63] Delaere, F., et al., 2013. The role of sodium-coupled glucose co-transporter 3 in the satiety effect of portal glucose sensing. Molecular Metabolism 2(1):47—53.

[64] Everard, A., et al., 2011. Responses of gut microbiota and glucose and lipid metabolism to prebiotics in genetic obese and diet-induced leptin-resistant mice. Diabetes 60(11):2775—2786.

[65] Habib, A.M., et al., 2012. Overlap of endocrine hormone expression in the mouse intestine revealed by transcriptional profiling and flow cytometry. Endocrinology 153(7):3054—3065.

[66] Cho, H.-J., et al., 2014. Differences in hormone localisation patterns of K and L type enteroendocrine cells in the mouse and pig small intestine and colon. Cell and Tissue Research 359(2):693—698.

[67] Spangeus, A., Forsgren, S., el-Salhy, M., 2000. Does diabetic state affect co-localization of peptide YY and enteroglucagon in colonic endocrine cells? Histology and Histopathology 15(1):37—41.

[68] Grunddal, K.V., et al., 2016. Neurotensin is coexpressed, coreleased, and acts together with GLP-1 and PYY in enteroendocrine control of metabolism. Endocrinology 157(1):176—194.

[69] Cho, H.-J., et al., 2014. Glucagon-like peptide 1 and peptide YY are in separate storage organelles in enteroendocrine cells. Cell and Tissue Research 357(1):63—69.

[70] Charney, A.N., Micic, L., Egnor, R.W., 1998. Nonionic diffusion of short-chain fatty acids across rat colon. American Journal of Physiology 274(3 Pt 1): G518—G524.

[71] Murphy, K.G., Bloom, S.R., 2006. Gut hormones and the regulation of energy homeostasis. Nature 444(7121):854—859.